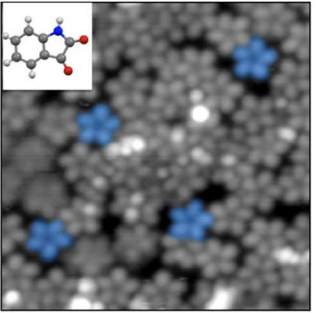


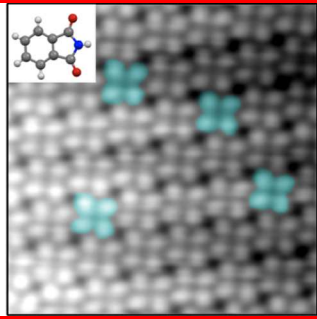
Scanning Tunneling Microscopy Investigation of Two-Dimensional Polymorphism of Structural Isomers

Angela M. Silski,[†] Jacob P. Petersen,[†] Ryan D. Brown,[‡] Steven A. Corcelli,[†] and S. Alex Kandel*,[†]

Supporting Information

Monolayers of two pairs of structural isomers were deposited on Au(111) and observed via scanning tunneling microscopy in ultrahigh vacuum. We observe exclusively cyclic pentamers of isatin (1H-indole-2,3-dione), whereas its structural isomer, phthalimide (isoindole-1,3dione), self-assembles primarily into close-packed arrays, with alternate structures that include kinetically locked disordered clusters and tetramer networks. Removal of the phthalimide NH group and its replacement with a CH₂ group produces 1,3-indandione, which, despite the loss of the hydrogen-bond donor site, self-assembles into similar structures: close-packed areas and tetramer networks. The equivalent analog for isatin,





1,2-indandione, does not form pentamers and instead forms only close-packed areas and disordered regions. By iteratively altering the chemical structure, we demonstrate the influence that the chemical structure has on the resulting two-dimensional

■ INTRODUCTION

In the fields of crystal engineering, supramolecular chemistry, and molecular self-assembly, the major goal is to demonstrate the fine control of molecular organization in one, two, and three dimensions. To achieve this goal, a fundamental understanding of how intermolecular interactions affect crystal packing is needed; studies of crystal packing in two dimensions can contribute to this understanding. Given the structurefunction relationship on the nanoscale, tailor-made nanostructures may result in new materials with desired physical and chemical properties. Two-dimensional (2D) nanostructures are of interest for use in molecular electronics, 2,3 host-guest systems, 4-6 optoelectronic devices such as organic field-effect transistors and organic light-emitting diodes, 8,9 and organic semiconductors.10

The design of a desired self-assembled monolayer can be achieved by carefully tuning both the noncovalent moleculemolecule interactions and the molecule-substrate interactions. 11-13 Many novel 2D supramolecular assemblies have been realized on metal surfaces via both covalent and noncovalent interactions, including metal-organic frameworks, ^{14,15} covalent—organic frameworks, ^{16,17} macrocyclic polymers, ¹⁸ quasicrystals, ^{19,20} molecular pentagonal stars, ²¹ and Archimedean tilings. ²² Scanning tunneling microscopy (STM) is a useful technique to study the 2D structure of such supramolecular assemblies because of its molecular and submolecular resolution. Given that STM is a local technique, it is useful in determining the structure of monolayers that exhibit structural polymorphism—information that may be lost

in ensemble surface characterization techniques. The combination of STM with density functional theory (DFT) calculations can be used to determine which noncovalent intermolecular interactions drive a particular 2D assembly.

There has been great interest in understanding how the chemical design of molecular building blocks, that is, the position and type of functional groups^{23,24} and the molecular geometry, 25,26 affects the resulting 2D supramolecular assembly. This remains a challenge, as a slight change in chemical structure may cause a drastic difference in the resulting 2D morphology. As a result, the ability to absolutely predict the 2D self-assembled structure that will result from a particular molecular building block on a particular surface has not yet been realized. The ability to predict an extended structure from the molecular structure would have implications in the controlled bottom-up design of nanostructures on surfaces as well as the controlled crystallization of particular polymorphs of three-dimensional (3D) crystals.

The indole backbone is abundant in many natural and synthetic products that are biologically active. Indolecontaining compounds have been the basis of pharmaceutical drugs with a variety of biological activities such as anticancer, antiviral, and antidepressant. The ability to predict the extended structure from molecular structure is of interest in drug design. Structural polymorphism is of particular interest

Received: August 23, 2018 Revised: October 9, 2018 Published: October 18, 2018

Department of Chemistry and Biochemistry, University of Notre Dame, Notre Dame, Indiana 46556, United States

^{*}Department of Chemistry and Biomolecular Science, Clarkson University, Potsdam, New York 13699, United States

The Journal of Physical Chemistry C

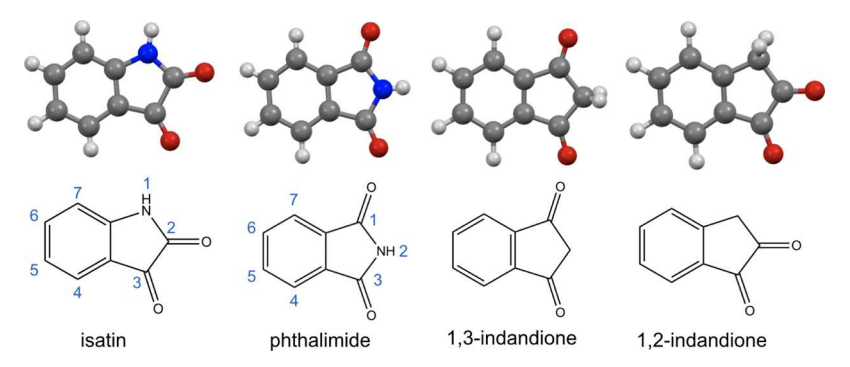


Figure 1. Chemical structures and 3D models of all molecules included in this study.

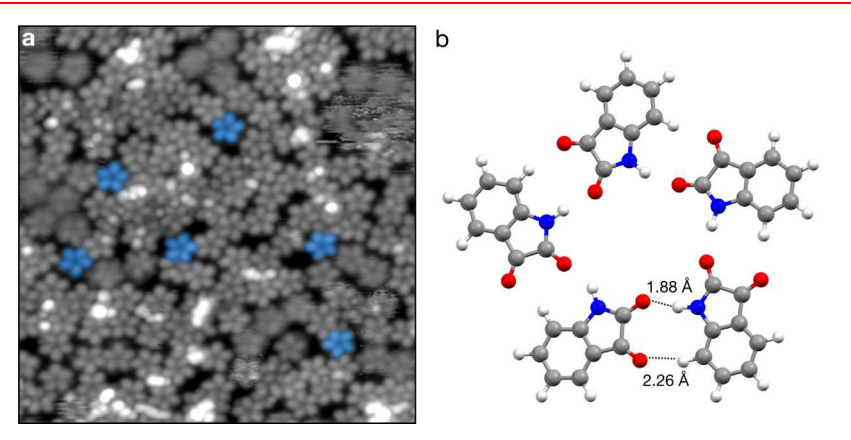


Figure 2. (a) STM topography image $(250 \times 250 \text{ Å})$ of isatin solution deposited in acetonitrile on Au(111) consists almost exclusively of pentamers (some representative structures highlighted in blue). (b) Optimized geometry of the isatin pentamer, showing that the N-H···O and C-H···O contacts contribute to stabilizing the pentamer. The calculated contact lengths of the N-H···O and C-H···O hydrogen bonds are shown.

to the pharmaceutical industry, as molecules in different polymorphs have different physical properties, such as solubility, and thus different bioavailability. Gaining a fundamental understanding of the intermolecular interactions of indole compounds may shed light on the role of intermolecular interactions in determining the extended structure in the solid state.

Here, we present an STM and DFT investigation of the 2D structures of indole diones and structural isomers, indandiones. We recently reported the observation of the cyclic pentamers of isatin (1H-indole-2,3-dione) stabilized by both N-H···O and C-H···O hydrogen bonds on an Au(111) surface.³² In this manuscript, we describe the surface self-assembly behavior of phthalimide, an isomer of isatin, on the Au(111) surface. We also describe the self-assembly of 1,2-indandione and 1,3indandione, the analogs of isatin and phthalimide, respectively, formed by replacing the NH with a CH2 group; all molecules are shown in Figure 1. Of these, only isatin forms cyclic pentamers; in contrast, all the other molecules exhibit, among other structures, a close-packed phase. We show that chemical structure plays a significant role in 2D self-assembled structures by systematically altering the chemical structure of the molecular building blocks.

An essential part of this investigation is the preparation of samples through exposure to both the gas-phase and solution-phase molecules. It is typical in ultrahigh vacuum experiments for adsorbates to be delivered to a surface through vacuum sublimation, which tends to produce highly ordered monolayers that reflect the thermodynamic ground state for the system. In contrast, pulsed deposition of molecules from

solution can produce both stable and metastable structures. Metastability is disadvantageous from the standpoint of engineering a surface monolayer with a single, well-defined structure; however, the ability to characterize one or more metastable states along with the ground state of the system can provide additional insights into how intermolecular interactions develop the structures of clusters and monolayers. The current study aims to maximize these insights through a combination of surface preparation techniques and the comparison of related molecules with similar structures.

METHODS

Scanning Tunneling Microscopy. Au(111)-on-mica substrates (Keysight Technologies) were cleaned in a high-vacuum chamber by three cycles of Ar⁺ sputtering (0.55 kV, 15 min) and annealing at 350–400 °C (15 min). The sample was allowed to cool before it was transferred to a high-vacuum load lock chamber. Droplets of 20 μ M solutions of the molecule of interest were delivered via a pulsed solenoid valve (Parker Instruments, Series 9, IOTA ONE Driver, 0.5 mm diameter nozzle) onto an Au(111) substrate kept at room temperature. The sample was then transferred to an Omicron LT-STM, kept at a base pressure of 5 × 10⁻¹⁰ Torr, and cooled to 77 K. All images were acquired with a Pt/Ir tip in constant current mode with a tunneling current of 10 pA and a tip—sample bias of +1.0 V.

Density Functional Theory. All structural optimizations were performed with the Q-Chem software package. These structures were optimized with the B3LYP global hybrid functional, chosen for its parameterization to model small

organic models. The 6-311++G(d,p) basis set was used, along with Grimme's D3 dispersion correction. In the generation of multimolecular structures, the structures were made with C_n symmetry, where n is the number of molecules in the structure. The structures were then optimized without any constraint in the gas phase. All the structures were subjected to the Boys and Bernardi counterpoise correction to account for the basis set superposition error.

RESULTS AND DISCUSSION

Isatin Pentamers. Five-lobed pentameric structures are the predominant species of isatin present on the Au(111) surface (Figure 2a). In addition, bright features are ascribed to the beginning of the second layer growth, and the blurry features (where the pentamer structure is less resolved, but still discernible) are characteristic of the clusters that are mobile on the surface and that move faster than the STM scan rate. The pentamers are cyclic, and the axis of each molecule points toward the center of each cluster.

The isatin pentamers are similar to the cyclic pentamers observed for indole-2-carboxylic acid³³ and ferrocenecarboxylic acid, 19 which are chiral upon adsorption on the Au(111) surface. In these studies, the molecules were deposited onto the surface from the droplets of solution pulsed into vacuum, and there is evidence for metastable cluster formation in solution as the result of the nonequilibrium rapid droplet evaporation process. 34,35 In contrast, the adsorption of molecules onto a surface from the gas phase is more likely to produce a minimum-energy structure. For indole-2carboxylic acid, pentamers and other metastable clusters formed as a result of solution deposition, 33 whereas an ordered catemer structure, representative of the solid-state crystal structure, formed as a result of vapor deposition of the same molecule.³⁶ Isatin is distinct in that it forms pentamers both from solution-based and gas-phase depositions, indicating that these structures are particularly stable on the gold surface.³² Isatin is the first case where we observed the anomalous pentamer structure as a result of both solution and vapor depositions of the same molecule; the pentamers also appear at both high and low surface coverages (Figure S1).

DFT has produced a bonding model for the isatin pentamer, as shown in Figure 2b. The pentamer is stabilized by the N-H...O hydrogen bonds between the nitrogen of the amine and the 2-position carbonyl oxygen and the C-H···O hydrogenbond contact between the aromatic proton at the 7-position and the carbonyl oxygen at the 3-position. The isatin pentamer cluster has a per-molecule binding energy of 52.9 kJ mol⁻¹, which is 16.9 kJ mol⁻¹ more stable than the binding energy of the isatin dimer. This bonding model was tested experimentally, as substitutions of a methyl group at the 3-position and fluorine at the 7-position of the aromatic ring precluded the C-H...O hydrogen bond, thus disrupting the cyclic pentamer.32

In the interest of testing our working model that adjacent hydrogen bonding sites on the five-membered ring of the indole heterocycle create a preference for cyclic pentamers, we investigated phthalimide, an isomer of isatin, in which the two carbonyl groups are no longer adjacent (structure is shown in Figure 1). The crystal structures of isatin and phthalimide are strikingly similar, with both the crystal structures based on the N-H···O dimer contacts supported by the C-H···O secondary contacts.^{37–39}

The DFT calculations produce an optimized geometry for the phthalimide cyclic pentamer, which is shown in Figure 3.

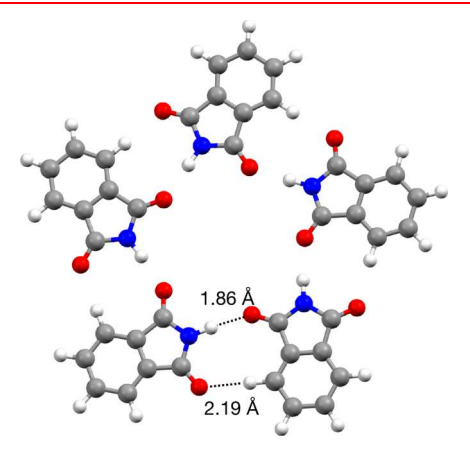


Figure 3. DFT-calculated optimized geometry for a phthalimide pentamer cluster. N-H···O and C-H···O contacts and their distances are shown between a pair of molecules.

There is a N-H···O hydrogen bond (1.86 Å) and C-H···O interaction (2.19 Å) that are slightly shorter than the contacts of the isatin pentamer cluster. The H···A (where A is the hydrogen bond acceptor) distances are typically 1.2-1.5 Å for strong, 1.5-2.2 Å for moderate, and greater than 2.2 Å for weak hydrogen bonds; 40 thus, the N-H···O and C-H···O interactions that are calculated could be classified as moderate and weak hydrogen-bond interactions, respectively.

The binding energy of the phthalimide pentamer is 45.4 kJ mol⁻¹, which is 15.6 kJ mol⁻¹ more stable than the calculated phthalimide dimer binding energy. Figure 4 shows a

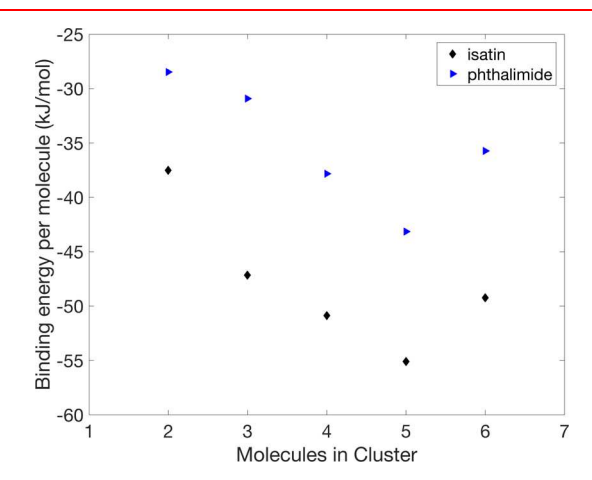


Figure 4. Plot of binding energy per molecule vs number of molecules in the cluster for isatin and phthalimide. Both molecules follow the same trend of decreasing binding energy with increasing cluster size; however, isatin overall exhibits more favorable (negative) binding energy than phthalimide for all clusters.

comparison of per-molecule binding energies for dimers through the pentamers of isatin and phthalimide. For both molecules, increasing the cluster size brings the 7-position aromatic proton closer to the 3-position carbonyl group to form an energetically favorable C-H···O hydrogen bond; steric hindrance begins with six-molecule clusters, where the C-H···O distance becomes too short.

The Journal of Physical Chemistry C

Monolayers of Phthalimide on Au(111). We expected to find that phthalimide, like isatin, forms pentamers on the Au(111) surface. Instead, STM images of solution-deposited phthalimide reveal close-packed ordered molecules as the majority species (Figure 5a). The underlying $22 \times \sqrt{3}$

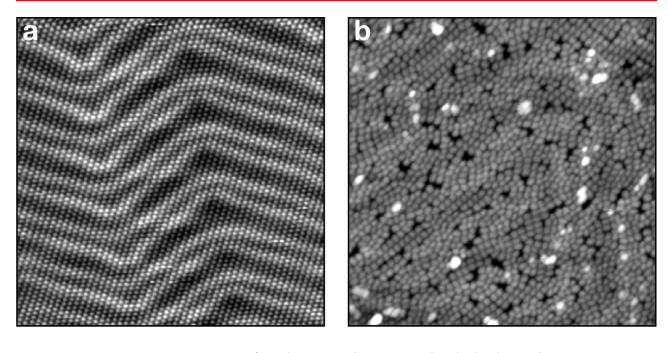


Figure 5. STM images of solution-deposited phthalimide in acetone on Au(111). (a) 400×400 Å area of close-packed molecules, where the underlying contrast represents the Au(111) surface reconstruction. (b) 350×350 Å area of disordered clusters of phthalimide molecules.

Au(111) herringbone is responsible for the contrast in the close-packed areas in Figure 5a. In addition, we observe disordered molecular clusters (Figure 5b) and some areas of tetrameric networks of molecules (Figure 6a,b).

A close-packed phase is unlikely to be the result of intermolecular hydrogen bonding, as a phthalimide molecule in a hexagonally packed region does not have enough hydrogen-bonding groups to make equivalent contacts to all

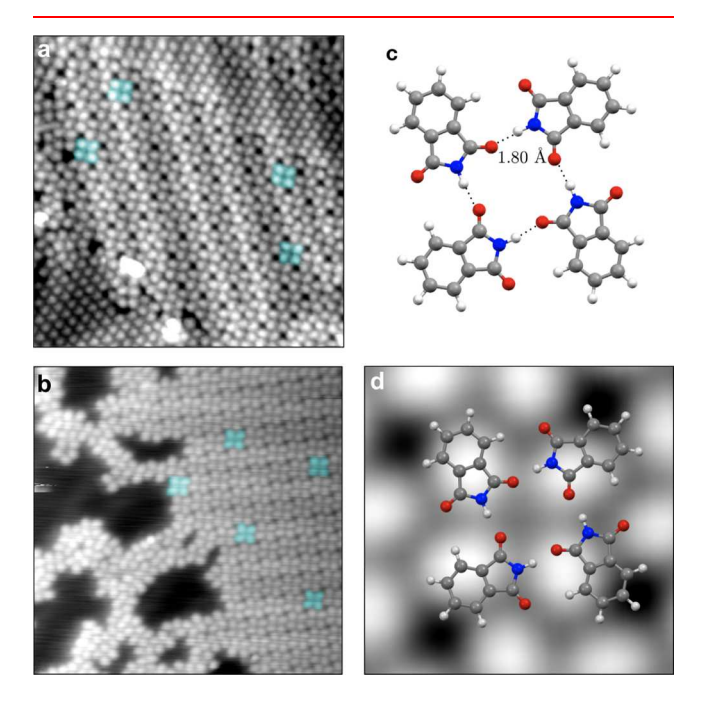


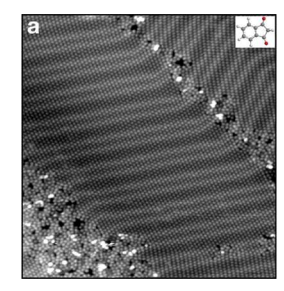
Figure 6. STM topography images of phthalimide tetramers. (a) 200 × 200 Å area of a tetramer network at 1 monolayer of surface coverage. (b) 220 × 220 Å area of lower coverage phthalimide tetramer networks. Representative tetramers are highlighted in blue. (c) DFT-optimized geometry of a cyclic tetramer, with the N-H···O contact distances shown. (d) Composite image of all tetramers shown in panel (b) (22 × 22 Å). Optimized geometry in panel (c) is overlaid.

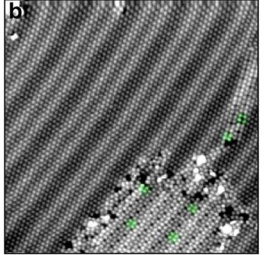
of its nearest neighbors. Instead, the data suggest a reduced importance of intermolecular interactions and a corresponding increased importance of molecule-surface interactions. In line with this, we note that the per-molecule binding energies for isatin clusters are lower than that for phthalimide across the range of cluster sizes that were calculated (Figure 4). This suggests that the hydrogen-bond strength between isatin molecules is stronger than that of phthalimide molecules. However, there is also some evidence that the phthalimidesurface interaction is weaker than the isatin-surface interaction. A phthalimide monolayer annealed at room temperature lost significant surface coverage (Figure S2a), which indicates a weaker molecule-substrate interaction, as the molecules were able to overcome the barriers to desorption at room temperature. The isatin monolayer did not lose surface coverage after thermal annealing at 40 $^{\circ}\text{C}$ (Figure S2b), and the majority of isatin pentamers remained intact.

The tetramer networks shown in Figure 6 are an interesting minority species, not only because they exhibit directional intermolecular interactions, but also because they are observed in solution-deposited but not vapor-deposited samples (Figure S3). This indicates that the tetramers are metastable. Our method of sample preparation involves the direct injection of the solvated molecule of interest into a vacuum chamber, and it involves rapidly evaporating and supercooling droplets. 41,42 Such a nonequilibrium environment may give rise to structures that may not be accessible at equilibrium conditions. We have shown that these nonequilibrium conditions can produce metastable 2D structures. 33-35,43 According to Ostwald's rule, 44 the least stable species will precipitate out first, potentially becoming kinetically locked on the surface. Although there are examples of solvent-controlled 2D polymorphism at the liquid-solid interface, 45-47 neither the phthalimide tetramer networks nor the isatin pentamers were solvent-dependent species (Figure S4).

It is important to emphasize that when considering metastable clusters or monolayer structures on the surface, there are three distinct states of the system to consider: the surface adsorbates as they come out of solution, the structures reached as the sample sits at room temperature for a short period of time, and the final structures observed in the experiment after the sample is cooled to 77 K. From the observation of the tetramer networks of phthalimide, only as the result of solution-based deposition, it is strongly argued that these structures are metastable. However, the possibility cannot be discounted that there could be other metastable structures that are formed initially and that anneal out at room temperature or that the formation of tetramer networks (or the tetramers themselves) occurs through the rearrangement of some other metastable species while the sample sits at room temperature or at some point in the cooling cycle. Performing pulse deposition onto a cooled sample would be one way to search for additional metastable structures, although the need to evaporate the solvent places a lower limit on the sample temperature.

The tetramers that we observe are well-ordered as a part of a network, similar to those quartet networks of xanthine (whose chemical structures are also five- and six-membered heterocycles) on Au(111),⁴⁸ which are stabilized solely by the strong N-H···O hydrogen bonds within and between the tetramers. However, it is unlikely that the networks of phthalimide tetramers are held together by hydrogen bonds because there are no feasible hydrogen-bond donors or acceptors on the The Journal of Physical Chemistry C





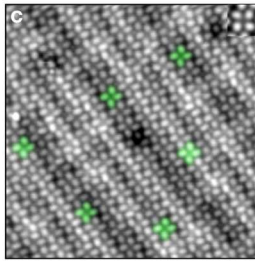


Figure 7. STM images of 1,3-indandione on Au(111) at 1 monolayer surface coverage. (a) 500 × 500 Å image of close-packed molecules and disordered clustering. (b) $400 \times 400 \text{ Å}$ area that contains both close-packed domains and tetramer networks. (c) $200 \times 200 \text{ Å}$ area composed of an extended tetramer network. Inset: Composite image of 108 tetramers in the image (c). Representative tetramer structures are highlighted in green.

outside of the molecule (on the six-membered ring) that could form hydrogen bonds to hold the network together. Each individual phthalimide tetramer looks similar to the 1naphthylmethylamine tetramers observed on Au(111), in which the amino groups are oriented in the center of each cluster; however, the 1-naphthylmethylamine tetramers that Feng et al.⁴⁹ observe do not exhibit any long-range order. It is possible that the phthalimide tetramer networks may be stabilized by weak van der Waals interactions, as there have been reported examples of such van der Waals-stabilized ordered networks assembled on surfaces.⁵⁰ In addition, it could be possible that molecules within a phthalimide tetramer are not planar on the surface and could be stabilized by $\pi-\pi$ stacking interactions. Although $\pi - \pi$ interactions are weak interactions, there are 2D assemblies that have been formed by the $\pi-\pi$ stacking interactions. 51,52 Although lower in energy than hydrogen bonding, the $\pi-\pi$ stacking interactions have been shown to compete with the hydrogen bonding interactions to drive the formation of self-assembled architectures.53

As seen in Figure 4, there is no local energy minimum for a cyclic N-H···O-bonded tetramer. In line with this, the DFToptimized geometry for the cyclic N-H···O-bonded phthalimide tetramer (Figure 6c,d) does not provide a good fit to the data. In particular, the DFT calculation predicts a structure that is too small to match the observed features; this is not a calibration error, as a good fit results when the calculated isatin pentamer is overlaid on the data (Figure S6).

It is also important to consider that the calculated binding energies are for planar gas-phase clusters. The measurements of the clusters' apparent topography show that the phthalimide close-packed phase and the tetramer networks appear equal in height, whereas the phthalimide tetramer appears roughly 50 pm taller than the isatin pentamer in STM images. Thus far, we have assumed that the isatin pentamer lies flat on the Au(111)surface; therefore, a taller phthalimide tetramer may indicate that the molecules in the cluster do not lie parallel to the surface.

The evidence presented thus far suggests that unlike isatin, phthalimide forms structures where N-H···O hydrogen bonding is less important or unimportant, and the structures formed are not planar. To test this, we study similar molecules in which N-H is removed and replaced with a CH2 group (structures shown in Figure 1). These analog molecules no longer involve a strong hydrogen-bond donor, and thus, would not be expected to form 2D hydrogen-bonded clusters.

Indandione Derivatives. Monolayers of 1,3-indandione were prepared by solution deposition in methanol on Au(111). The STM images reveal that at 1 monolayer surface coverage,

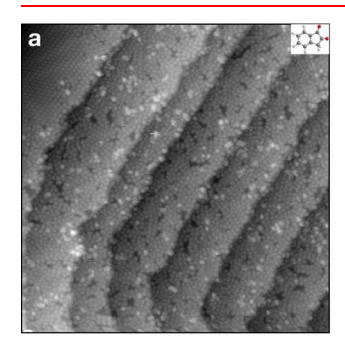
there is a mixture of close-packed ordered molecules and disordered clustering (Figure 7a) and close-packed tetramer networks that match those of phthalimide (Figure 7b,c). The inset of Figure 7c shows a composite image of 108 tetramers and reveals that the structure of the tetramer involves molecules that point toward the center of the molecule. This tetramer network appears identical to the tetramer network that appears in Figure 6a,b.

Although the structure of 1,3-indandione in Figure 1 has no strong hydrogen-bond donors, tautomerization to the ketoenol form of the molecule migrates one of the CH2 hydrogens to the adjacent C=O, forming an OH functional group that can then participate in hydrogen bonding. It is possible that the 1,3-indandione tetramers are O-H···O hydrogen-bonded cyclic structures. Furthermore, we extend this to phthalimide and propose that this molecule also tautomerizes. The tautomerization of these molecules explains the observation that N-H···O hydrogen bonding appears less important for phthalimide and also explains the dramatic differences between phthalimide and isatin.

β-Diketones commonly exhibit keto—enol tautomerism. The diketo forms of both phthalimide⁵⁴ and 1,3-indandione⁵⁵ are the prevalent species in the gas phase; however, 1,3-indandione has been known to exhibit significant tautomerization to the keto-enol form in dimethyl sulfoxide, a highly polar solvent. 55 There is evidence that the gas-phase form of a molecule may not be the species that adsorbs on a metal surface. Although it has been well-established that deprotonation of carboxyl groups can occur upon adsorption on the more reactive Cu(111) substrate, 56-58 anthraquinone-2-carboxylic acid is known to chemisorb on gold in the carboxylate form.⁵⁹ In addition to carboxyl-containing molecules, there has been some evidence of structural changes of amines upon interaction with metal surfaces. Uracil, also a 1,3-dione with an amine group at the 2-position, has been shown to be energetically unstable in its enol tautomer form in the gas phase.⁶⁰ However, uracil has been shown to have strong molecule-substrate interactions with various surfaces that may change the structure of the molecule upon surface adsorption: deprotonation upon adsorption on Cu(111),⁶¹ coordination to the surface with both O atoms and the N atom, 62 and chemisorption on Au(111),⁶³ Au(110),⁶⁴ Au(100),⁶⁵ and Ag(111).66 Upon adsorption on the Au(110) surface, it has been shown that the enol form of uracil is preferred over the keto form by as much as 22 kJ mol⁻¹.64 Therefore, the gasphase calculated structure may not be the structure that adsorbs on a surface, as the interaction with metal surfaces may result in structural changes to the adsorbate.

The compound 1,3-Indandione exhibits positive solvatochromism, that is, the absorption of light is red-shifted with increasing solvent polarity. A 1,3-indandione solution is orange when dissolved in toluene, whereas when dissolved in methanol, the solution is purple. Keto-enol tautomerism, which involves the shift of a π bond, may alter the π -electronic structure of a molecule and thus may significantly alter the chemical and physical properties of the molecule. There are some examples of molecules that exhibit solvatochromic shifts in the visible region that occur as a result of keto-enol tautomerism. ⁶⁷⁻⁶⁹ Given that 1,3-indandione is known to exhibit solvent-dependent tautomerization to the enol form in polar solvents, 55 we infer that the shift in the keto-enol equilibrium of 1,3-indandione to the enol form is evidenced by the visible color change in highly polar solvents. To test the dependence of the solvent on the resulting 2D structure, monolayers of 1,3-indandione were prepared in toluene. It is expected that the diketo form of 1,3-indandione would be favored in toluene. However, the surface-supported structures do not appear to be solvent-dependent, as the monolayers are similar when prepared in methanol and toluene (Figure S5). This result shows that the solvent polarity is not a driving force for stabilizing the enol form upon adsorption on a surface. It could be plausible that the interaction with the surface drives the molecule to its enol form to form a O-H···O tetramer.

As a confirmation of our model for the isatin pentamer, we elected to prepare monolayers of 1,2-indandione, in which N—H is removed from isatin and replaced with CH₂. The result is quite different from that of isatin, as the pentamer formation is completely blocked (Figure 8). Monolayers of 1,2-indandione



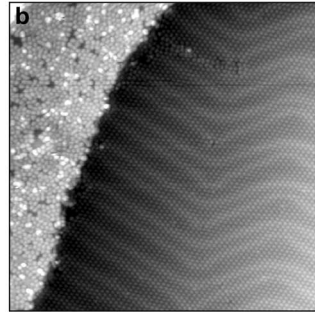


Figure 8. STM topography images of 1,2-indandione reveal: (a) disordered clustering on step edges and (b) close-packed molecules. Image sizes = 500×500 Å.

consist of disordered clusters and arrays of close-packed molecules. Given that our DFT model for the isatin pentamer involves primary N-H···O contacts and secondary C-H···O contacts (Figure 2b), it is unsurprising that the removal of the primary hydrogen-bond donor prevents the formation of pentamers. The results of the 1,2-indandione experiments on Au(111) confirm the importance of the N-H···O hydrogen bond in the isatin pentamer—without this primary hydrogen-bonded contact, pentamer formation is precluded. For the case of phthalimide and 1,3-indandione, removal of the N-H···O contact results in no change in the surface-supported structures. Thus, we conclude that the phthalimide tetramer structure is not dependent on the N-H···O hydrogen bond for formation.

CONCLUSIONS

In summary, we have investigated the effect that the hydrogenbond donor/acceptor position has on the formation of unique 2D structures of isomers of indole diones and indandiones on the Au(111) surface. Isatin forms almost exclusively cyclic pentamers stabilized by N-H···O and C-H···O hydrogen bonds, whereas its structural isomer, phthalimide, results in a mixture of close-packed molecules, disordered clusters, and tetrameric networks. DFT binding energy calculations do not support the formation of phthalimide tetramers, as there is no energy well for a four-molecule cluster. The optimized geometry produced by DFT suggests a cyclic N-H···O hydrogen-bonded tetramer. We probed the role of N-H as a hydrogen-bond donor in the formation of both the isatin pentamer and the phthalimide tetramers. Removal of N-H from phthalimide and replacing it with CH2 to make 1,3indandione results in no drastic change in the structure of the monolayer, and tetramer formation is preserved. Unsurprisingly, the removal of N-H from isatin completely precludes pentamer formation, reinforcing the importance of the N-H··· O contact in the stabilization of the isatin pentamer. This study illustrates the strong influence that the position of hydrogenbond donor and acceptor sites has on the resulting assembled monolayers.

ASSOCIATED CONTENT

S Supporting Information

The Supporting Information is available free of charge on the ACS Publications website at DOI: 10.1021/acs.jpcc.8b08221.

STM images of low-coverage isatin on Au(111); thermal annealing experiments; vapor deposition of phthalimide on Au(111); isatin, phthalimide, and 1,3-indandione pulse deposited in different solvents; and an overlaid model of the isatin pentamer on experimental STM data (PDF)

AUTHOR INFORMATION

Corresponding Author

*E-mail: skandel@nd.edu.

ORCID (

Steven A. Corcelli: 0000-0001-6451-4447 S. Alex Kandel: 0000-0001-8191-1073

Notes

The authors declare no competing financial interest.

ACKNOWLEDGMENTS

This research was supported by funding from the National Science Foundation (NSF grant nos. CHE-1507213 and CHE-1807313).

REFERENCES

- (1) Mali, K. S.; Pearce, N.; De Feyter, S.; Champness, N. R. Frontiers of supramolecular chemistry at solid surfaces. *Chem. Soc. Rev.* **2017**, *46*, 2520–2542.
- (2) Hoeben, F. J. M.; Jonkheijm, P.; Meijer, E. W.; Schenning, A. P. H. J. About Supramolecular Assemblies of π -Conjugated Systems. *Chem. Rev.* **2005**, *105*, 1491–1546.
- (3) Xiang, D.; Wang, X.; Jia, C.; Lee, T.; Guo, X. Molecular-scale electronics: From concept to function. *Chem. Rev.* **2016**, *116*, 4318–4440
- (4) Phillips, A. G.; Perdigão, L. M. A.; Beton, P. H.; Champness, N. R. Tailoring pores for guest entrapment in a unimolecular surface self-

- assembled hydrogen bonded network. Chem. Commun. 2010, 46,
- (5) Li, S.; Huang, J.; Zhou, F.; Cook, T. R.; Yan, X.; Ye, Y.; Zhu, B.; Zheng, B.; Stang, P. J. Self-assembly of triangular and hexagonal molecular necklaces. J. Am. Chem. Soc. 2014, 136, 5908-5911.
- (6) Iritani, K.; Tahara, K.; De Feyter, S.; Tobe, Y. Host-Guest Chemistry in Integrated Porous Space Formed by Molecular Self-Assembly at Liquid-Solid Interfaces. Langmuir 2017, 33, 4601-4618.
- (7) Tseng, T.-C.; Urban, C.; Wang, Y.; Otero, R.; Tait, S. L.; Alcamí, M.; Écija, D.; Trelka, M.; Gallego, J. M.; Lin, N.; et al. Chargetransfer-induced structural rearrangements at both sides of organic/ metal interfaces. Nat. Chem. 2010, 2, 374-379.
- (8) Khassanov, A.; Steinrück, H.-G.; Schmaltz, T.; Magerl, A.; Halik, M. Structural investigations of self-assembled monolayers for organic electronics: Results from x-ray reflectivity. Acc. Chem. Res. 2015, 48, 1901-1908.
- (9) Chua, L.-L.; Zaumseil, J.; Chang, J.-F.; Ou, E. C.-W.; Ho, P. K.-H.; Sirringhaus, H.; Friend, R. H. General observation of n-type fieldeffect behaviour in organic semiconductors. Nature 2005, 434, 194-199.
- (10) Rancatore, B. J.; Mauldin, C. E.; Tung, S.-H.; Wang, C.; Hexemer, A.; Strzalka, J.; Fréchet, J. M. J.; Xu, T. Nanostructured organic semiconductors via directed supramolecular assembly. ACS Nano 2010, 4, 2721-2729.
- (11) Bartels, L. Tailoring molecular layers at metal surfaces. Nat. Chem. 2010, 2, 87-95.
- (12) Hirsch, B. E.; McDonald, K. P.; Flood, A. H.; Tait, S. L. Living on the edge: Tuning supramolecular interactions to design twodimensional organic crystals near the boundary of two stable structural phases. J. Chem. Phys. 2015, 142, 101914.
- (13) Slater, A. G.; Perdigão, L. M. A.; Beton, P. H.; Champness, N. R. Surface-based supramolecular chemistry using hydrogen bonds. Acc. Chem. Res. 2014, 47, 3417-3427.
- (14) Langner, A.; Tait, S. L.; Lin, N.; Chandrasekar, R.; Ruben, M.; Kern, K. Ordering and Stabilization of Metal-Organic Coordination Chains by Hierarchical Assembly through Hydrogen Bonding at a Surface. Angew. Chem., Int. Ed. 2008, 47, 8835-8838.
- (15) Dong, L.; Gao, Z.; Lin, N. Self-assembly of metal-organic coordination structures on surfaces. Prog. Surf. Sci. 2016, 91, 101-
- (16) Liu, X.-H.; Guan, C.-Z.; Ding, S.-Y.; Wang, W.; Yan, H.-J.; Wang, D.; Wan, L.-J. On-Surface Synthesis of Single-Layered Two-Dimensional Covalent Organic Frameworks via Solid-Vapor Interface Reactions. J. Am. Chem. Soc. 2013, 135, 10470-10474.
- (17) Mo, Y.-P.; Liu, X.-H.; Wang, D. Concentration-directed polymorphic surface covalent organic frameworks: Rhombus, parallelogram, and kagome. ACS Nano 2017, 11, 11694-11700.
- (18) Steiner, C.; Gebhardt, J.; Ammon, M.; Yang, Z.; Heidenreich, A.; Hammer, N.; Görling, A.; Kivala, M.; Maier, S. Hierarchical onsurface synthesis and electronic structure of carbonyl-functionalized one- and two-dimensional covalent nanoarchitectures. Nat. Commun. 2017, 8, 14765.
- (19) Wasio, N. A.; Quardokus, R. C.; Forrest, R. P.; Lent, C. S.; Corcelli, S. A.; Christie, J. A.; Henderson, K. W.; Kandel, S. A. Selfassembly of hydrogen-bonded two-dimensional quasicrystals. Nature 2014, 507, 86-89.
- (20) Urgel, J. I.; Écija, D.; Lyu, G.; Zhang, R.; Palma, C.-A.; Auwärter, W.; Lin, N.; Barth, J. V. Quasicrystallinity expressed in twodimensional coordination networks. Nat. Chem. 2016, 8, 657-662.
- (21) Stöckl, Q.; Bandera, D.; Kaplan, C. S.; Ernst, K.-H.; Siegel, J. S. Gear-Meshed Tiling of Surfaces with Molecular Pentagonal Stars. J. Am. Chem. Soc. 2014, 136, 606-609.
- (22) Zhang, Y.-Q.; Paszkiewicz, M.; Du, P.; Zhang, L.; Lin, T.; Chen, Z.; Klyatskaya, S.; Ruben, M.; Seitsonen, A. P.; Barth, J. V.; et al. Complex supramolecular interfacial tessellation through convergent multi-step reaction of a dissymmetric simple organic precursor. Nat. Chem. 2018, 10, 296-304.

- (23) Brown, R. D.; Corcelli, S. A.; Kandel, S. A. Structural polymorphism as the result of kinetically controlled self-assembly. Acc. Chem. Res. 2018, 51, 465-474.
- (24) Bouju, X.; Mattioli, C.; Franc, G.; Pujol, A.; Gourdon, A. Bicomponent Supramolecular Architectures at the Vacuum-Solid Interface. Chem. Rev. 2017, 117, 1407-1444.
- (25) Furukawa, S.; Uji-i, H.; Tahara, K.; Ichikawa, T.; Sonoda, M.; De Schryver, F. C.; Tobe, Y.; De Feyter, S. Molecular Geometry Directed Kagomé and Honeycomb Networks: Toward Two-Dimensional Crystal Engineering. J. Am. Chem. Soc. 2006, 128, 3502-3503.
- (26) Ishikawa, D.; Ito, E.; Han, M.; Hara, M. Effect of the steric molecular structure of azobenzene on the formation of self-assembled monolayers with a photoswitchable surface morphology. Langmuir 2013, 29, 4622-4631.
- (27) Fu, C.; Rosei, F.; Perepichka, D. F. 2D self-assembly of fused oligothiophenes: molecular control of morphology. ACS Nano 2012, 6, 7973-7980.
- (28) Hu, Y.; Miao, K.; Zha, B.; Xu, L.; Miao, X.; Deng, W. STM investigation of structural isomers: alkyl chain position induced selfassembly at the liquid/solid interface. Phys. Chem. Chem. Phys. 2016,
- (29) Hu, Y.; Miao, K.; Xu, L.; Zha, B.; Miao, X.; Deng, W. Effects of alkyl chain number and position on 2D self-assemblies. RSC Adv. 2017, 7, 32391-32398.
- (30) Kaushik, N.; Kaushik, N.; Attri, P.; Kumar, N.; Kim, C.; Verma, A.; Choi, E. Biomedical importance of indoles. Molecules 2013, 18, 6620-6662.
- (31) Zhang, M.-Z.; Chen, Q.; Yang, G.-F. A review on recent developments of indole-containing antiviral agents. Eur. J. Med. Chem. 2015, 89, 421-441.
- (32) Silski, A. M.; Brown, R. D.; Petersen, J. P.; Coman, J. M.; Turner, D. A.; Smith, Z. M.; Corcelli, S. A.; Poutsma, J. C.; Kandel, S. A. C-H···O Hydrogen Bonding in Pentamers of Isatin. J. Phys. Chem. C 2017, 121, 21520-21526.
- (33) Wasio, N. A.; Quardokus, R. C.; Brown, R. D.; Forrest, R. P.; Lent, C. S.; Corcelli, S. A.; Christie, J. A.; Henderson, K. W.; Kandel, S. A. Cyclic hydrogen bonding in indole carboxylic acid clusters. J. Phys. Chem. C 2015, 119, 21011-21017.
- (34) Quardokus, R. C.; Wasio, N. A.; Brown, R. D.; Christie, J. A.; Henderson, K. W.; Forrest, R. P.; Lent, C. S.; Corcelli, S. A.; Alex Kandel, S. Hydrogen-bonded clusters of 1, 1'-ferrocenedicarboxylic acid on Au(111) are initially formed in solution. J. Chem. Phys. 2015, 142, 101927.
- (35) Brown, R. D.; Coman, J. M.; Christie, J. A.; Forrest, R. P.; Lent, C. S.; Corcelli, S. A.; Henderson, K. W.; Kandel, S. A. Evolution of Metastable Clusters into Ordered Structures for 1,1'-Ferrocenedicarboxylic Acid on the Au(111) Surface. J. Phys. Chem. C 2017, 121, 6191-6198.
- (36) De Marchi, F.; Cui, D.; Lipton-Duffin, J.; Santato, C.; MacLeod, J. M.; Rosei, F. Self-assembly of indole-2-carboxylic acid at graphite and gold surfaces. J. Chem. Phys. 2015, 142, 101923.
- (37) Zakaria, C. M.; Low, J. N.; Glidewell, C. Phthalimide at 120 K: Perforated molecular ribbons containing three different ring motifs. Acta Crystallogr., Sect. C: Cryst. Struct. Commun. 2002, 58, 09-010.
- (38) Palmer, M. H.; Blake, A. J.; Gould, R. O. 14N nuclear quadropole coupling in cyclic amides and thioamides. Ab initio simulations of the solid state environment as interpretation of the NQR spectra of 2-pyridinone, isatin and benzothiazolezone. A new Xray structure for isatin. I. Chem. Phys. 1987, 115, 219-227.
- (39) Palenik, G. J.; Koziol, A. E.; Katritzky, A. R.; Fan, W.-Q. Nonbonded interactions. The influence of lone pair repulsions on bond lengths. J. Chem. Soc., Chem. Commun. 1990, 715-716.
- (40) Steiner, T. The hydrogen bond in the solid state. Angew. Chem., Int. Ed. 2002, 41, 48-76.
- (41) Smith, J. D.; Cappa, C. D.; Drisdell, W. S.; Cohen, R. C.; Saykally, R. J. Raman thermometry measurements of free evaporation from liquid water droplets. J. Am. Chem. Soc. 2006, 128, 12892-12898.

- (42) Drisdell, W. S.; Saykally, R. J.; Cohen, R. C. On the evaporation of ammonium sulfate solution. *Proc. Natl. Acad. Sci. U.S.A.* **2009**, *106*, 18897–18901.
- (43) Brown, R. D.; Quardokus, R. C.; Wasio, N. A.; Petersen, J. P.; Silski, A. M.; Corcelli, S. A.; Kandel, S. A. Non-intuitive clustering of 9,10-phenanthrenequinone on Au(111). *Beilstein J. Nanotechnol.* **2017**, *8*, 1801–1807.
- (44) Threlfall, T. Structural and Thermodynamic Explanations of Ostwald's Rule. Org. Process Res. Dev. 2003, 7, 1017–1027.
- (45) Gatti, R.; MacLeod, J. M.; Lipton-Duffin, J. A.; Moiseev, A. G.; Perepichka, D. F.; Rosei, F. Substrate, molecular structure, and solvent effects in 2D self-assembly via hydrogen and halogen bonding. *J. Phys. Chem. C* 2014, *118*, 25505–25516.
- (46) Mamdouh, W.; Uji-I, H.; Ladislaw, J. S.; Dulcey, A. E.; Percec, V.; De Schryver, F. C.; De Feyter, S. Solvent controlled self-assembly at the liquid-solid interface revealed by STM. *J. Am. Chem. Soc.* **2005**, 128, 317–325.
- (47) Sirtl, T.; Song, W.; Eder, G.; Neogi, S.; Schmittel, M.; Heckl, W. M.; Lackinger, M. Solvent-dependent stabilization of metastable monolayer polymorphs at the liquid-solid interface. *ACS Nano* **2013**, 7, 6711–6718.
- (48) Chen, C.; Sang, H.; Ding, P.; Sun, Y.; Mura, M.; Hu, Y.; Kantorovich, L. N.; Besenbacher, F.; Yu, M. Xanthine quartets on Au(111). J. Am. Chem. Soc. 2018, 140, 54–57.
- (49) Feng, Z.; Castellarin Cudia, C.; Floreano, L.; Morgante, A.; Comelli, G.; Dri, C.; Cossaro, A. A competitive amino-carboxylic hydrogen bond on a gold surface. *Chem. Commun.* **2015**, *51*, *5739*–5742.
- (50) Iritani, K.; Ikeda, M.; Yang, A.; Tahara, K.; Hirose, K.; Moore, J. S.; Tobe, Y. Hexagonal molecular tiling by hexagonal macrocycles at the liquid/solid interface: Structural effects on packing geometry. *Langmuir* **2017**, *33*, 12453–12462.
- (51) Beniwal, S.; Chen, S.; Kunkel, D. A.; Hooper, J.; Simpson, S.; Zurek, E.; Zeng, X. C.; Enders, A. Kagome-like lattice of π - π stacked 3-hydroxyphenalenone on Cu(111). *Chem. Commun.* **2014**, *50*, 8659–8662.
- (52) Jethwa, S. J.; Kolsbjerg, E. L.; Vadapoo, S. R.; Cramer, J. L.; Lammich, L.; Gothelf, K. V.; Hammer, B.; Linderoth, T. R. Supramolecular corrals on surfaces resulting from aromatic interactions of nonplanar triazoles. *ACS Nano* **2017**, *11*, 8302–8310.
- (53) Gutzler, R.; Lappe, S.; Mahata, K.; Schmittel, M.; Heckl, W. M.; Lackinger, M. Aromatic interaction vs. hydrogen bonding in self-assembly at the liquid-solid interface. *Chem. Commun.* **2009**, 680–682
- (54) Ackera, A.; Hofmann, H.-J.; Cimiraglia, R. On the tautomerism of maleimide and phthalimide derivatives. *J. Mol. Struct.: THEO-CHEM* **1994**, *315*, 43.
- (55) Sigalov, M. V. Keto-Enol Tautomerism of Phenindione and Its Derivatives: An NMR and Density Functional Theory (DFT) Reinvestigation. *J. Phys. Chem. A* **2015**, *119*, 1404–1414.
- (56) Fischer, S.; Papageorgiou, A. C.; Lloyd, J. A.; Oh, S. C.; Diller, K.; Allegretti, F.; Klappenberger, F.; Seitsonen, A. P.; Reichert, J.; Barth, J. V. Self-assembly and chemical modifications of bisphenol A on Cu(111): Interplay between ordering and thermally activated stepwise deprotonation. *ACS Nano* **2014**, *8*, 207–215.
- (57) Steiner, C.; Gliemann, B. D.; Meinhardt, U.; Gurrath, M.; Meyer, B.; Kivala, M.; Maier, S. Self-assembly and stability of hydrogen-bonded networks of bridged triphenylamines on Au(111) and Cu(111). *J. Phys. Chem. C* **2015**, *119*, 25945–25955.
- (58) Schmitt, T.; Hammer, L.; Schneider, M. A. Evidence for On-Site Carboxylation in the Self-Assembly of 4,4'-Biphenyl Dicarboxylic Acid on Cu(111). *J. Phys. Chem. C* **2016**, 120, 1043–1048.
- (59) Han, S. W.; Joo, S. W.; Ha, T. H.; Kim, Y.; Kim, K. Adsorption characteristics of anthraquinone-2-carboxylic acid on gold. *J. Phys. Chem. B* **2000**, *104*, 11987–11995.
- (60) Orozco, M.; Hernández, B.; Luque, F. J. Tautomerism of 1-methyl derivatives of uracil, thymine, and 5-bromouracil. Is tautomerism the basis for the mutagenicity of 5-bromouridine? *J. Phys. Chem. B* **1998**, *102*, 5228–5233.

- (61) Papageorgiou, A. C.; Fischer, S.; Reichert, J.; Diller, K.; Blobner, F.; Klappenberger, F.; Allegretti, F.; Seitsonen, A. P.; Barth, J. V. Chemical transformations drive complex self-assembly of uracil on close-packed coinage metal surfaces. *ACS Nano* **2012**, *6*, 2477–2486.
- (62) Duncan, D. A.; Unterberger, W.; Kreikemeyer-Lorenzo, D.; Woodruff, D. P. Uracil on Cu(110): A quantitative structure determination by energy-scanned photoelectron diffraction. *J. Chem. Phys.* **2011**, *135*, 014704.
- (63) Dretschkow, T.; Dakkouri, A. S.; Wandlowski, T. In-situ scanning tunneling microscopy study of uracil on Au(111) and Au(100). *Langmuir* 1997, 13, 2843–2856.
- (64) Irrera, S.; de Leeuw, N. H. A density functional theory study of the adsorption of uracil on the Au(100) surface. *Proc. R. Soc. A* **2011**, 467, 1959–1969.
- (65) Irrera, S.; Roldan, A.; Portalone, G.; De Leeuw, N. H. The role of hydrogen bonding and proton transfer in the formation of uracil networks on the gold (100) surface: A density functional theory approach. *J. Phys. Chem. C* **2013**, *117*, 3949–3957.
- (66) Cavallini, M.; Aloisi, G.; Bracali, M.; Guidelli, R. An in situ STM investigation of uracil on Ag(111). *J. Electroanal. Chem.* **1998**, 444, 75–81.
- (67) Furuta, H.; Ishizuka, T.; Osuka, A.; Dejima, H.; Nakagawa, H.; Ishikawa, Y. NH tautomerism of N-confused porphyrin. *J. Am. Chem. Soc.* **2001**, *123*, 6207–6208.
- (68) Holschbach, M. H.; Sanz, D.; Claramunt, R. M.; Infantes, L.; Motherwell, S.; Raithby, P. R.; Jimeno, M. L.; Herrero, D.; Alkorta, I.; Jagerovic, N.; et al. Structure of a 4-nitroso-5-aminopyrazole and its salts: Tautomerism, protonation, and E/Z isomerism. *J. Org. Chem.* **2003**, *68*, 8831–8837.
- (69) Yamashita, H.; Abe, J. Remarkable solvatochromic color change via proton tautomerism of a phenol-linked imidazole derivative. *J. Phys. Chem. A* **2014**, *118*, 1430–1438.